

KfK 3240  
April 1982

# **The Stability of NbTi Composite Superconductors of High Cu / SC-Ratio**

P. Turowski, L. Z. Lin  
Institut für Technische Physik

**Kernforschungszentrum Karlsruhe**



KERNFORSCHUNGSZENTRUM KARLSRUHE

Institut für Technische Physik

KfK 3240

The Stability of NbTi Composite Superconductors  
of High Cu/SC - Ratio

P. Turowski, L.Z. Lin<sup>+</sup>)

Kernforschungszentrum Karlsruhe GmbH, 7500 Karlsruhe

<sup>+</sup>) Institute of Electrical Engineering, Academia Sinica,  
Peking, China

Als Manuskript vervielfältigt  
Für diesen Bericht behalten wir uns alle Rechte vor

Kernforschungszentrum Karlsruhe GmbH  
ISSN 0303-4003

## Abstract

Investigations with respect to stability behaviour were made on NbTi composite multifilamentary conductors of a Cu/SC ratio of 10 in magnetic field from 7 T up to 10 T. The recovery currents in dependence on the magnetic field were determined under bath cooling conditions at 4.2 K for a heat disturbance of 0.6 Joule. The current sharing regime turned out to be very extended due to the high copper content and consequently offered a safety margin in magnets in case of transient overcurrents. The copper stabilizer was attached to the superconductor in different ways but the stability behaviour was not changed.

## Zusammenfassung

### Die Stabilität von NbTi Verbundsupraleitern mit hohem Cu/SL-Verhältnis

Untersuchungen des Stabilitätsverhalten wurden an NbTi-Multifilament-Verbundleitern mit einem Cu/SL-Verhältnis von 10 im Feldbereich zwischen 7 und 10 T gemacht. Es wurden die Recovery-Ströme in Abhängigkeit vom Magnetfeld bei Kühlung im Heliumbad von 4.2 K nach einem Wärmepuls mit 0,6 Joule bestimmt. Wegen des hohen Anteils an Kupfer im Leiter war der "current sharing" Bereich sehr ausgedehnt und bot damit bei transienten Stromüberschreitungen eine Sicherheitsreserve. Das stabilisierende Kupfer war am Supraleiter auf verschiedene Weisen angebracht, aber das Stabilitätsverhalten war davon nicht beeinträchtigt.

## 1. Introduction

For a large magnet project in China a NbTi Superconductor with a copper matrix of Cu/SC ratio of 10 and a size of  $3.6 \times 7 \text{ mm}^2$  was proposed. To determine the most economical manufacturing process, three types of conductors were compared: one monolithic conductor and two composite conductors, where NbTi-conductors of small size and low copper content were soldered into U shaped copper strips. This was the largest superconductor made in China up to now. A 35 cm diameter bore superconducting solenoid generating a magnetic field of 3.5 T was built in 1979 by the Institute of Electrical Engineering of Academia Sinica using these different conductor configurations in a pancake structure. It was of particular interest to compare the performance of these conductors with respect to critical current and the stability behaviour in high magnetic fields. The critical current, the take-off current, the recovery current and the current sharing behaviour of these conductors were determined using the equipment and the technique<sup>1)</sup> at the ITP (Institute of Technical Physics) of Kernforschungszentrum Karlsruhe.

## 2. The conductor configurations

The main parameters of the conductor are given in the following;

Size	$3.6 \times 7 \text{ mm}^2$
Filament diameter	$\sim 70 \text{ }\mu\text{m}$
Number of filaments	432
Twist pitch	120 mm
Cu/SC ratio	10

Fig. 1 shows the schematic cross section of the monolithic conductor and the arrangement of the grooves provided for cooling channels. The grooves are rolled into the surface of the conductor and have therefore wide tolerances with respect to the nominal depth of 0.5 mm.

Fig. 2 shows the schematic cross sections of the two other conductor configurations. The arrangement of grooves is the same as above.

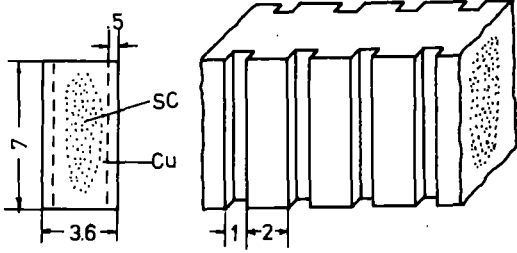


Fig. 1 The schematic cross section of the monolithic conductor

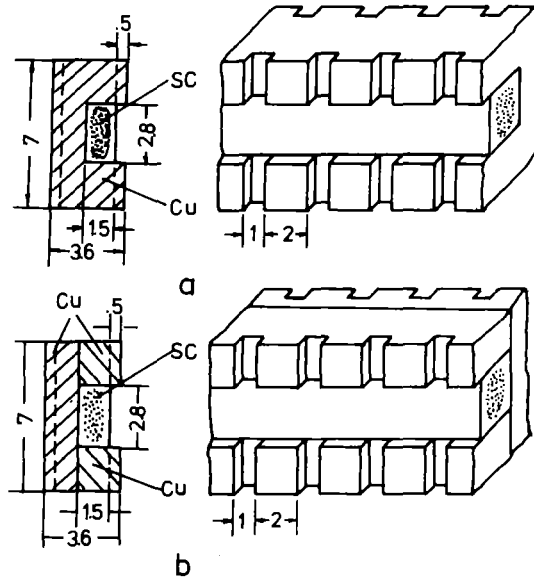


Fig. 2 The schematic cross sections of the two composite conductors

In case a, the superconductor soldered into the U-shaped copper strip has a size of  $1.5 \times 2.8 \text{ mm}^2$ . 432 filaments of  $70 \text{ }\mu\text{m}$  diameter are embedded in a copper matrix of  $\text{Cu}/\text{SC} = 1$  and are twisted with a pitch of 12 cm. In case b, the U shaped copper strip consists of three parts which are soldered together with the same superconductor applied by lead-tin solder.

The stabilizing copper should have OFHC quality, indicated by the manufacturer, but the residual resistivity ratio (RRR) has only a value of 70. A certain reduction in the residual resistivity ratio may be caused by the cold working on the conductor. The magnetoresistance of the copper matrix at different magnetic fields could be measured when the superconductor was completely in the normal conducting stage. Slightly above the recovery current the superconductor could be transferred into a steady normal conducting stage by a heat pulse. Variation of the transport current in this situation gives an Ohmic increase of voltage with a straight U-I-line that may be extrapolated through the origin. Due to the negligible temperature dependence of copper resistivity below about 20 K, the variation in conductor temperature due to changing transport current does not influence the measurement of magnetoresistance. Fig. 3 illustrates the magnetoresistance effect of the copper used compared to one of RRR 154. The difference in the absolute values of resistivity is practically given by the initial values, whereas the linear increase in the magnetic field is the same in both cases, giving a slope of  $0.45 \times 10^{-10} \text{ }\Omega\text{m}/\text{T}$ .

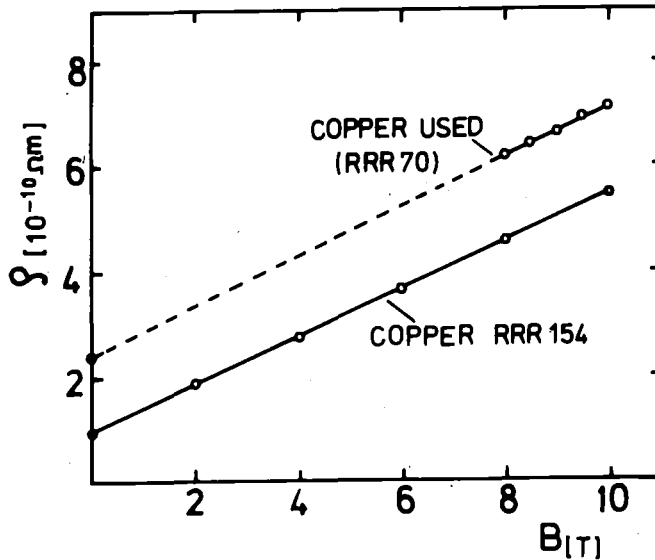


Fig. 3 The magnetoresistance effect of the copper used

### 3. Experimental set-up

The background superconducting magnet used for this experiment was a NbTi/Nb<sub>3</sub>Sn solenoid magnet system with a clear bore of 100 mm diameter. The maximum field at the sample position (radius  $r = 45$  mm) was 10.5 T. The conductor samples were wound spirally onto a coil former of 90 mm diameter and 30 mm length. A heater of 0.1 mm diameter manganin wire was wound bifilarly around the conductor and then thermally insulated by a layer of epoxy resin. With several potential taps along the conductor, growth and collapse of a normal conducting zone could be observed. From the voltage amplitude, the extension of the normal zone could be determined. Cooling channels at the upper and lower surfaces of the conductors guaranteed a good thermal contact to the liquid helium.

### 4. Stability behaviour of the conductors

Fig. 4 shows the critical current  $I_C$ , take-off current  $I_{t.o.}$  and recovery current  $I_R$  of the monolithic conductor in dependence on the magnetic field from 7 T to 10 T. The critical current  $I_C$  was defined for a voltage drop of 0.2  $\mu\text{V}$  per cm conductor length. The take-off current  $I_{t.o.}$  is that current in the current sharing

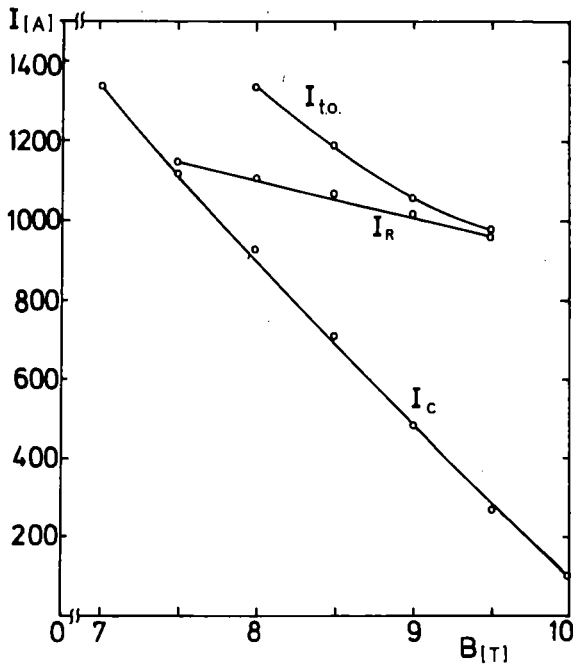


Fig. 4  
Critical current  $I_c$ , take-off current  $I_{t.o.}$  and recovery current  $I_R$  of monolithic conductor in dependence on the magnetic field  $B$ .

regime, at which the superconducting stage breaks down completely by lack of cooling power or internal processes in the superconductor.

The measurements on recovery current  $I_R$  were performed in the following way: A heat pulse of 10 msec duration was applied to the conductor by the heater and the pulse current generator. The input energy is about 0.6 J resulting in an estimated temperature of the conductor of about 30 K over a length of 2-3 mm. The transport current was raised after each heat pulse till the superconductor turned normal conducting. The recovery current is the limit of current at which the superconducting stage is restored after an excursion into normal conductivity.

The experiments have shown that the recovery current  $I_R$  is smaller than the critical current in the magnetic fields below 7.5 T. The recovery current is found in the region between critical current and take-off current in magnetic fields higher than 8 T.

The Maddock stability criterion<sup>3)</sup>

$$q_e \geq \frac{\rho(B) \cdot I^2}{A \cdot \eta \cdot P}$$

is used as a measure of stability.  $q_e$  is the effective heat flow rate,  $W/cm^2$ ,  $\rho(B)$  is the resistivity of the Cu-stabilized conductor,  $\Omega m$ ,  $A$  is the cross section of the stabilizer,  $cm^2$ ,  $\eta$  ( $= 0.56$  for the monolithic conductor and  $0.64$  for the composite) is the liquid helium wetted fraction of the surface and  $P$  is the perimeter of the conductor,  $cm$ . The effective heat flow rate  $q_e$  can be calculated if the current  $I$  is replaced by the recovery current  $I_R$ . In table 1, the calculated values of the effective heat flow rate  $q_e$  of the composite conductor are given in different magnetic fields.

The values of the effective heat flow are somewhat smaller than from other measurements with the same nominal cooling channel geometry<sup>4)</sup>. It must be mentioned again that the cooling channels in the present case have certain deviations in the depth due to the manufacturing process resulting in an average depth somewhat smaller than  $0.5$  mm. This may be the explanation for the deviation from usual values.

B [T]	7.5	8	8.5	9	9.5
$q_e [Wcm^{-2}]$	0.328	0.315	0.309	0.286	0.263

Table 1: The effective heat flow rates  $q_e$  in dependence on the magnetic field B.

As in other cases, the effective heat flow increases with decreasing magnetic field even though the magnetoresistance effect is taken into account.

Table 2 shows that there is nearly no difference between dynamically and steadily measured recovery currents. The dynamic recovery currents  $I_R$  are those which are determined by apply-

B [T]	8	8.5	9	9.5
$I_{SR} [A]$	1130	1080	1000	940
$I_R [A]$	1110	1070	1020	960

Table 2: The steady and the dynamic recovery currents  $I_{SR}$ ,  $I_R$  in dependence on the magnetic field B.

ing a local heat pulse to introduce a transient normal conducting zone; they are shown in Fig. 4. Recovery of a completely normal conducting sample by reducing the transport current slowly is called stationary recovery. The stationary recovery currents  $I_{SR}$  are determined in the way, that normal conductivity in the total sample was introduced by a heat pulse at a transport current just above the dynamic recovery current. The current was then reduced to that point where the sample returns into the superconducting stage. In general, this stationary recovery current is somewhat smaller than the dynamic recovery current.

The Fig. 5 shows the critical current  $I_c$ , take-off current  $I_{t.o.}$  and recovery current  $I_R$  in dependence on the magnetic

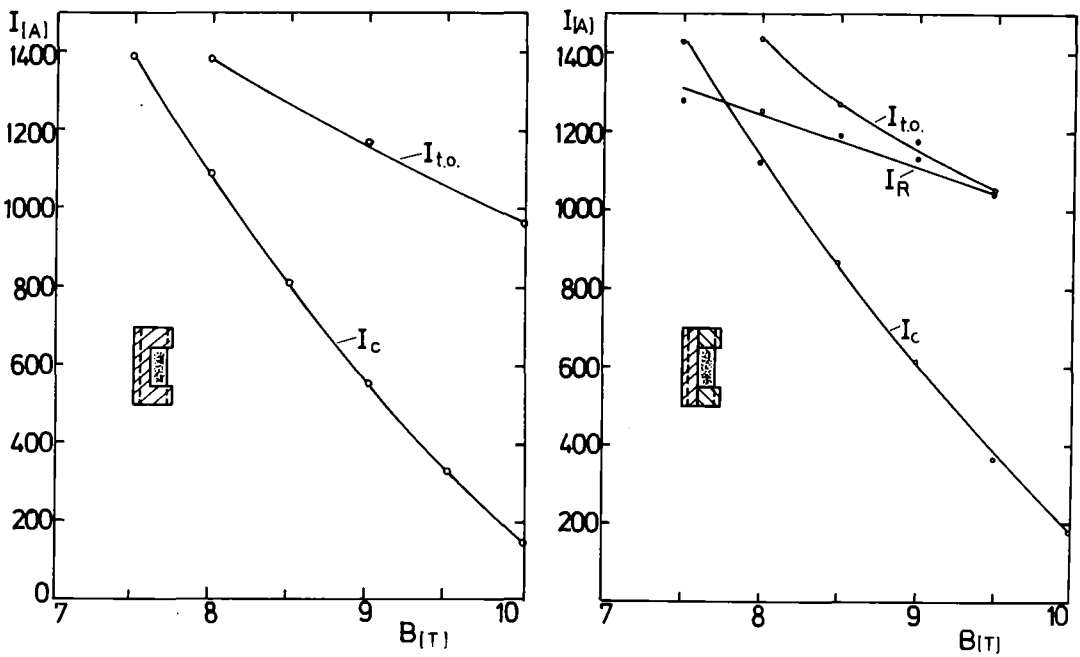


Fig. 5 The characteristics of both soldered composite conductors

field for the both soldered composite conductors. There is nearly no difference in the performance compared to the monolithic conductor.

### 5. The current sharing behaviour

Because the investigated superconductors have a high Cu/Sc ratio, they show a distinct current sharing behaviour in parti-

cular in high magnetic fields, i.e. at small current densities. The Fig. 6 demonstrates the behaviour for the monolithic NbTi-conductor at 8 T. The transition into the complete normal conducting stage at the take-off point is not determined by the limited cooling power, because the recovery into the supercon-

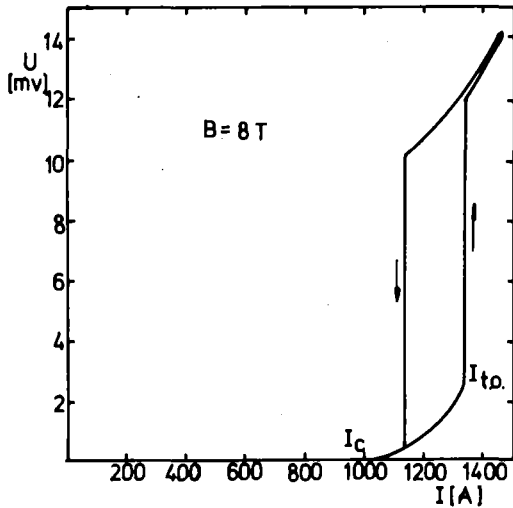


Fig. 6  
The quench and recovery process of the monolithic NbTi-conductor in 1 turn

ducting stage sets in at a higher power level during reduction of the transport current. Rather it must be supposed, that intrinsic processes depending on the current density are finally responsible for the change from the superconducting to the normal conducting stage. In a very high magnetic field a nearly smooth transition from the superconducting to the normal conducting stage can be observed as Fig. 7 shows. This behaviour has been observed before<sup>5)</sup>.

As is well known the current sharing is caused by the appearance of resistivity in the superconductor, i.e. the NbTi, due to flux flow when the transport current is exceeding the critical current. In that case the superconductor behaves like a normal conductor and a current sharing with the normal conducting matrix sets in. By means of the voltage-current characteristic and the resistance of the matrix it is possible to calculate the partial currents in the matrix and the superconductor, and consequently also the resistivity of the superconductor can be determined.

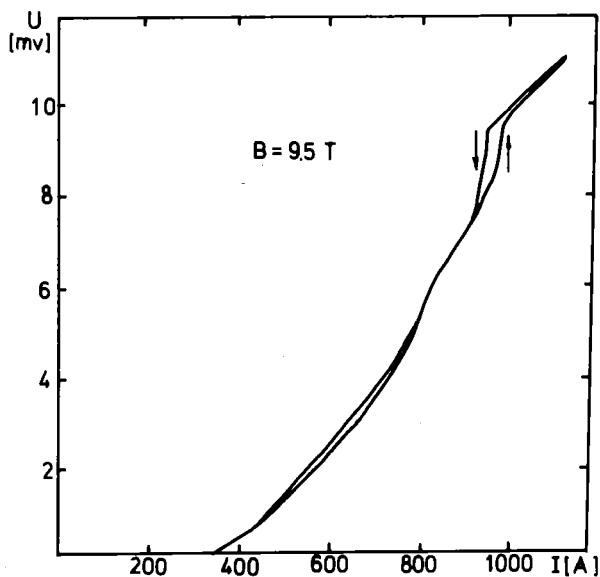


Fig. 7 The transition between normal and superconducting stages for the monolithic NbTi-conductor at  $B = 9.5 \text{ T}$

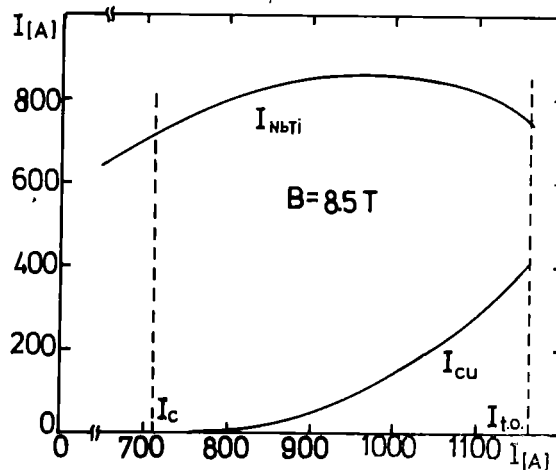


Fig. 8 Current distribution in monolithic conductor between the NbTi and the copper at  $B = 8.5 \text{ T}$

In Fig. 8 the current distribution in the monolithic conductor between the NbTi and the copper matrix is given versus the transport current up to the take-off point. The current in the matrix increases continuously, whilst the current in the superconductor passes a maximum value. The decrease of the current in the NbTi can be explained by a temperature enhancement in the whole conductor due to Joule dissipation.

In Table 3 the current distribution between NbTi and copper for different magnetic fields is given at the take-off point.

$B_{[T]}$	8	8.5	9	9.5
$I_{to}[A]$	1340	1160	1060	980
$I_{Cu}[A]$	273	410	806	857
$I_{sc}[A]$	1067	750	254	123

Table 3:

Current distribution between copper and superconductor at the take-off point for various magnetic fields.

With decreasing magnetic field, i.e. with increasing critical current density in the NbTi, the bypass current in the matrix becomes smaller. That means the resistivity of the NbTi in the resistive stage depends on the current density and achieves in low magnetic fields at high current densities only smaller values before the superconducting stage collapses, as it is shown in Fig. 9.

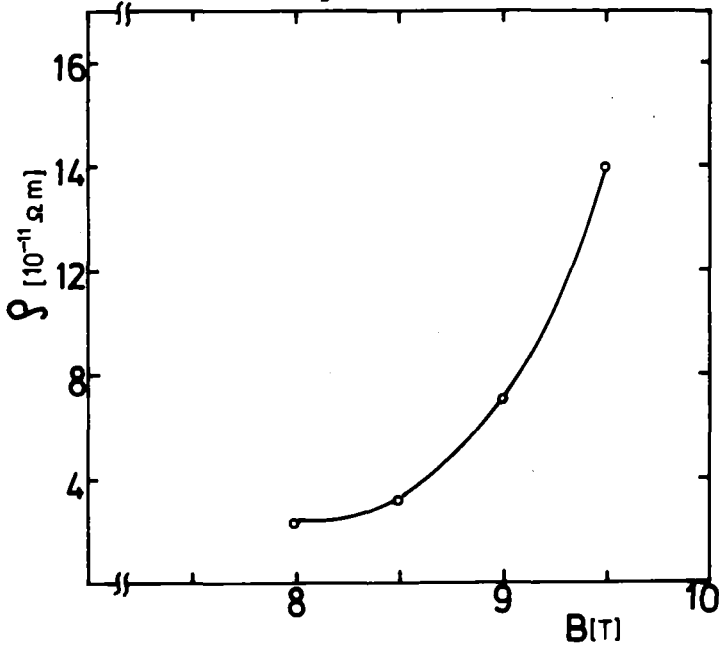


Fig. 9 The resistivity of NbTi in the resistive stage

A comparison of the current sharing behaviour at 8 T of the three investigated composite conductors is demonstrated in Fig. 10. The monolithic conductor shows a very smooth increase of voltage in the current sharing regime, whereas the current sharing of the two other composites, where the real supercon-

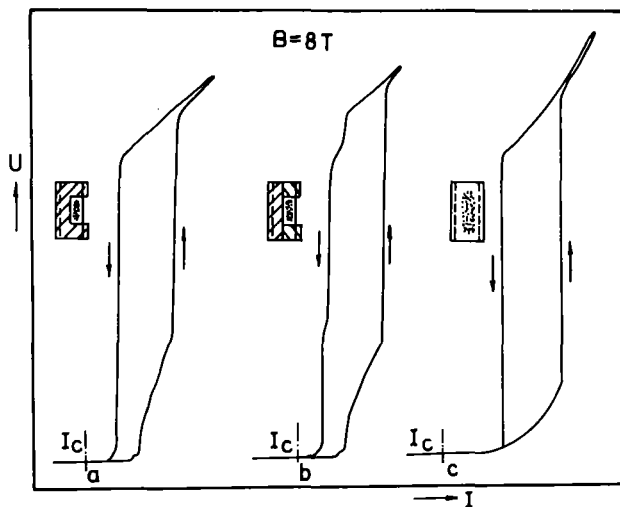


Fig. 10 The current sharing behaviour of the three investigated conductor types

ductor was soldered into a U-shaped copper strip, is characterized by a peculiarly shaped curvature. It can be assumed, that the change in curvature is caused by the bond resistance between the superconductor and the matrix.

## 6. Summary

The experiments have shown that the monolithic and the soldered composite NbTi conductors have the same recovery currents for applied pulsed heat disturbances. The cooling channels at the surface of the conductors allow an effective heat flow rate of more than  $0.3 \text{ W/cm}^2$  in fields less than 8.5 T. At a field of 7.5 T the recovery current equals the critical current, i.e. at that field the conductor behaves cryogenically stable. Because of the high copper content there is an extended current sharing regime which offers a marginal safety in case of overcurrents. The current sharing regime reveals certain differences in the current sharing behaviour of a monolithic and of soldered composite conductors.

## 7. References

- 1) Turowski, P.,  
The stability of Nb<sub>3</sub>Sn-composite conductors cooled by normal and superfluid helium,  
Cryogenics 21, 533 (1981).
- 2) Turowski, P., Lin, L.Z., Seibt, E.,  
Cu- and Al-stabilized Nb<sub>3</sub>Sn-multifilamentary conductors and their stability against heat pulses under bath cooling conditions,  
IEEE, MAG-17, 2047 (1981).
- 3) Maddock, B.J. et al.,  
Superconductive composites: Heat Transfer and steady state stabilization,  
Cryogenics 9, 261 (1969).
- 4) Turowski, P.,  
A Review on stability experiments with superconductors in liquid helium under pool boiling conditions,  
to be published by Int. Inst. of Refrigeration.
- 5) Gauster, W.F.,  
Steady-state performance of multistrand superconducting compound conductors,  
J. Appl. Phys. 40, 2060 (1969).